

# 1 **Effect of mid-term drought on *Quercus pubescens* BVOCs** 2 **emissions seasonality and their dependence to light and/or** 3 **temperature**

4 Amélie Saunier<sup>1</sup>, Elena Ormeño<sup>1</sup>, Christophe Boissard<sup>2</sup>, Henri Wortham<sup>3</sup>, Brice Temime-  
5 Roussel<sup>3</sup>, Caroline Lecareux<sup>1</sup>, Alexandre Armengaud<sup>4</sup>, Catherine Fernandez<sup>1</sup>.

6 <sup>1</sup>Aix Marseille Univ, Univ Avignon, CNRS, IRD, IMBE, Marseille, France.

7 <sup>2</sup>Laboratoire des Sciences du Climat et de l'Environnement, LSCE/IPSL, CEA-CNRS-UVSQ, Université Paris-  
8 Saclay, F-91191 Gif-sur-Yvette, France.

9 <sup>3</sup>Aix Marseille Univ, CNRS, LCE, Laboratoire de Chimie de l'Environnement, Marseille, France

10 <sup>4</sup> Air PACA, 146 rue Paradis, Bâtiment Le Noilly Paradis, 13294 Marseille, Cedex 06.

11 *Correspondence to:* Amélie Saunier (amelie.saunier@imbe.fr)

12 **Key words:** BVOCs, natural and amplified drought, season, light and temperature

13 **Abstract.** Biogenic volatile organic compounds (BVOCs) emitted by plants represent a large source of carbon  
14 compounds released into the atmosphere where they account for precursors of tropospheric ozone and secondary  
15 organic aerosols. Being directly involved in air pollution and indirectly in climate change, understanding what  
16 factors drive BVOC emissions is a prerequisite for modelling their emissions and predict air pollution. The main  
17 algorithms currently used to model BVOCs emissions are mainly light and/or temperature dependent. Additional  
18 factors such as seasonality and drought also influence isoprene emissions, especially in the Mediterranean region  
19 which is characterized by a rather long drought period in summer. These factors are increasingly included in  
20 models but only for the principal studied BVOC, namely isoprene but there are still some discrepancies in  
21 estimations of emissions. In this study, the main BVOCs emitted by *Quercus pubescens*: isoprene, methanol,  
22 acetone, acetaldehyde, formaldehyde, MACR, MVK and ISOPOOH (these 3 last compounds detected under the  
23 same m/z), were monitored with a PTR-ToF-MS over an entire seasonal cycle, under both *in situ* natural and  
24 amplified drought which is expected with climate change. Amplified drought impacted all studied BVOCs by  
25 reducing emissions in spring and summer while increasing emissions in autumn. All six BVOCs monitored showed  
26 daytime light and temperature dependencies while three BVOCs (methanol, acetone and formaldehyde) also  
27 showed emissions during the night despite the absence of light under constant temperature. Moreover, methanol  
28 and acetaldehyde burst in the early morning and formaldehyde deposition/uptake were also punctually observed  
29 which were not assessed by the classical temperature and light models.

## 30 **1 Introduction**

31 Plants contribute to global emissions of volatile organic compounds (VOCs) with an estimated emission rate of  
32  $10^{15}$  gC yr<sup>-1</sup> (Guenther *et al.* 1995; Harrison *et al.* 2013). The large variety of compounds released by plants  
33 represents, at the global scale, 2-3% of the total carbon released in the atmosphere (Kesselmeier & Staudt 1999).  
34 Under strong photochemical conditions, BVOCs, together with NO<sub>x</sub>, can significantly contribute to tropospheric  
35 ozone concentration (Xie *et al.* 2008; Papiez *et al.* 2009). In addition to its greenhouse effect, O<sub>3</sub> has strong effects  
36 on plant metabolism (Reig-Armiñana *et al.* 2004; Beauchamp *et al.* 2005) as well as on human health (Lippmann  
37 1989). BVOCs are also rapidly oxidized by OH radical and NO<sub>3</sub> (Hallquist *et al.* 2009; Liu *et al.* 2012), which  
38 account for an important fraction of the total mass of secondary organic aerosols (SOA, Jimenez *et al.* 2009).  
39 Methanol and acetone are, after isoprene, the principal BVOC released to the atmosphere. Isoprene emissions  
40 represent between 400-600 TgC yr<sup>-1</sup> at the global scale (Arneeth *et al.* 2008) whereas methanol emissions vary  
41 between 75 and 280 TgC yr<sup>-1</sup> (Singh *et al.* 2000; Heikes *et al.* 2002, respectively) and acetone emissions represent  
42 only 33 TgC yr<sup>-1</sup> (Jacob *et al.* 2002). Other compounds such as acetaldehyde, methacrolein (MACR), methyl vinyl  
43 ketone (MVK), isoprene hydroxy hydroperoxides (ISOPOOH) and formaldehyde, whose biogenic origin has been  
44 poorly investigated, are better known to be anthropogenic and/or secondary VOCs issued from atmospheric  
45 oxidations (Hallquist *et al.* 2009). However, acetaldehyde is also a by-product of plant metabolism and its  
46 emissions represent 23 Tg yr<sup>-1</sup> at the global scale (Millet *et al.* 2010). Formaldehyde, MACR, MVK and ISOPOOH  
47 are released by plants through oxidations of methanol and isoprene, respectively, within leaves but they can have  
48 other leaf precursors (Oikawa & Lerdau 2013). Thus, it is thereby important to model all this panel of BVOCs  
49 emissions with the aim of predicting their effect on secondary atmospheric chemistry.

50 Current models allow to predict BVOCs emissions according to the type of vegetation, biomass density, leaf age,  
51 specific emission factor for many vegetal species, as well as the impact of some environmental factors. Models,  
52 such as the MEGAN (Guenther *et al.* 2006; Guenther *et al.* 2012) or CHIMERE (Menuet *et al.* 2014) model, include  
53 at least two main algorithms that allow to model light and temperature emissions dependence (called *L+T*  
54 algorithm afterwards) and a temperature dependent algorithm (called *T* algorithm afterwards), both described in  
55 Guenther *et al.* (1995). The *L+T* algorithm is typically used for BVOCs emissions whose synthesis rapidly relies  
56 on photosynthesis, and hence include *de novo* emissions. The *T* algorithm is used for BVOCs emissions that do  
57 not directly rely on BVOCs synthesis when, for example, they originate from permanent large storage pools  
58 (Ormeno *et al.* 2011). The dependence to light and/or temperature is well documented for isoprenoids (Owen *et al.*  
59 2002; Rinne *et al.* 2002; Dindorf *et al.* 2006) but there is still a lack of knowledge about highly volatile BVOCs  
60 (e.g. methanol, acetone, acetaldehyde). However, many of these compounds are very reactive in the atmosphere  
61 (Hallquist *et al.* 2009) and, could be emitted in large quantities to the atmosphere at global scale. The  
62 characterization of their emissions and sensitivity to light and/or temperature is, thus, necessary in order to obtain  
63 reliable predictions of atmospheric processes in order not to miss this important part of the atmospheric reactivity.

64 Other factors than light and temperature can drive BVOCs emissions such as water stress. Most studies dealing  
65 with BVOCs response to water stress have, however, focused on terpene-like compounds and have been carried  
66 out after weeks of watering restriction or removal under controlled conditions (for a review, see studies cited in  
67 Peñuelas and Staudt 2010). Considerable uncertainty remains in our understanding of emission mechanisms since  
68 some works showed increases (Funk *et al.* 2004; Monson *et al.* 2007) or decreases of isoprene emissions  
69 (Brüggemann & Schnitzler 2002; Fortunati *et al.* 2008) and there is a lack of knowledge on the impact of water  
70 stress on highly volatile BVOCs emissions (e.g. methanol). Moreover, the understanding of isoprene sensitivity

71 and highly volatile BVOCs to recurrent water stress (few years) under *in situ* conditions is clearly missing.  
72 Likewise, the capacity of current L+T and T algorithms to predict emission shifts under different drought scenarios  
73 in the context of climate change needs to be addressed for isoprene and highly volatile compounds. This is of  
74 especial interest for the Mediterranean area where the most severe climatic scenario of the IPCC predicts an  
75 intensification of summer drought consisting on a rain reduction that can locally reach 30%, an extension of the  
76 drought period as well as a temperature rise of 3.4°C, (Giorgi & Lionello 2008; IPCC 2013; Polade *et al.* 2014)  
77 for 2100.

78 In the present investigation, we aimed (i) to study the emission factors of each studied BVOC released by *Q.*  
79 *pubescens*, including isoprene and highly volatile compounds that originate from plant metabolism under water  
80 stress (ii) to test the performance of the L+T and T algorithms to predict isoprene and highly volatile BVOC  
81 emissions over the seasonal cycle and under two recurrent water stress treatments. *Q. pubescens* was chosen as  
82 vegetal model because this species is highly resistant to drought and well widespread in the Northern  
83 Mediterranean area occupying 2 million ha (Quézel & Médail 2003). It also represents the major source of isoprene  
84 emissions in the Mediterranean area and the second one at the European scale (Keenan *et al.* 2009).

## 85 **2 Material and methods**

### 86 **2.1 Experimental site**

87 Our study was performed at the O<sub>3</sub>HP site (Oak Observatory at OHP, Observatoire de Haute Provence), located  
88 60 km North of Marseille, France (5°42'44" E, 43°55'54" N), at an elevation of 650m above the sea level. The  
89 O<sub>3</sub>HP (955m<sup>2</sup>), free from direct human disturbance for 70 years, is a homogeneous forest mainly composed of *Q.*  
90 *pubescens* (≈ 90 % of the biomass and ≈ 75 % of the trees) with a mean diameter of 1.3 m. The remaining 10 %  
91 of the biomass is mostly represented by *Acer monspessulanum* trees, a very low isoprene-emitter species (Genard-  
92 Zielinski *et al.* 2015). The O<sub>3</sub>HP site was created in 2009 in order to study the impact of climate change on a *Q.*  
93 *pubescens* forest. Using a rainfall exclusion device (an automated monitored roof deployed during chosen rain  
94 events) set up over part of the O<sub>3</sub>HP canopy, it was possible to reduce natural rain by 30% and to extend the  
95 drought period in an attempt to mimic the current climatic model projections for 2100 (Giorgi & Lionello 2008;  
96 IPCC 2013; Polade *et al.* 2014). Two plots were considered in the site; a plot receiving natural precipitation where  
97 trees grew under natural drought (300m<sup>2</sup> surface, used as control plot) and a second plot submitted to amplified  
98 drought (232m<sup>2</sup> surface). Rain exclusion on this latter plot started on May 2012 and was continuously applied  
99 every year, principally, during the growth period. Ombrothermic diagrams indicate that the drought period was  
100 extended for 2 months in 2012, 4 months in 2013 and 3 months in 2014 for amplified drought relative to natural  
101 drought (Fig 1). Data on cumulative precipitation show that 35% of rain was excluded in 2012 (from 29 April from  
102 to 27 October), 33.5% in 2013 (from 7 July from to 29 December), 35.5% in 2014 (from 8 April to 8 December).  
103 This experimental set up involved a recurrent drought in the amplified drought plot. Sampling was performed at  
104 the branch-scale at the top of the canopy during three campaigns from October 2013 to July 2014, covering an  
105 entire seasonal cycle: in autumn (14 to 28 October 2013, 2<sup>nd</sup> year of amplified drought), in spring (12 to 19 May  
106 2014, 3<sup>rd</sup> year of amplified drought) and in summer (13 to 25 July 2014, 3<sup>rd</sup> year of amplified drought). Spring,  
107 summer and autumn campaigns corresponded to the end of leaf growth, leaf maturation and the beginning of the  
108 leaf senescence, respectively. The same five trees per plot were selected and investigated throughout the study.

## 109 2.2 Branch scale-sampling methods

110 Two identical dynamic branch enclosures were used for sampling gas exchange (in terms of CO<sub>2</sub>, H<sub>2</sub>O and  
111 BVOCs) as fully described in Genard-Zielinski *et al.* (2015) with some modifications. Branches were enclosed in  
112 a  $\approx$  30L PTFE (polytetrafluoroethylene) frame closed by a 50 $\mu$ m thick PTFE film. One tree from natural and one  
113 tree from amplified drought plot were analysed concomitantly during 1 or 2 days. Inlet air was introduced at  
114 9L.min<sup>-1</sup>, controlled by mass flow controllers (MFC, Bronkhorst), using a pump, inside, by PTFE (KNF  
115 N840.1.2FT.18®, Germany) allowing for air renewal inside the chamber every  $\sim$  3min. Ozone was removed from  
116 inlet air by placing PTFE filters impregnated with sodium thiosulfate (Na<sub>2</sub>S<sub>2</sub>O<sub>3</sub>) as described by Pollmann *et al.*  
117 (2005), so that oxidation of BVOCs due to ozone within the enclosed atmosphere is negligible. The excess of air  
118 humidity was removed using drierite. A PTFE fan ensured a rapid mixing of the chamber air and a slight positive  
119 pressure within the enclosure enabled the PTFE film to be held away from leaves to minimise biomass damage.  
120 Microclimate (temperature, relative humidity and photosynthetically active radiation or PAR) was continuously  
121 (every minute) monitored by a data logger (LI-COR 1400®; Lincoln, NE, USA) with a relative humidity and  
122 temperature probe placed inside the chamber (RHT probe, HMP60, Vaisala, Finland) and a quantum sensor (PAR,  
123 LI-COR, PAR-SA 190®, Lincoln, NE, USA) placed outside the chamber. The climatic conditions in terms of PAR  
124 and temperatures are summarized in Fig. S1 (in supplementary files) for each field campaigns. All air flow rates  
125 were controlled by mass flow controllers (MFC, Bronkhorst) and all tubing lines were made of PTFE. Chambers  
126 were installed the day before measurements and flushed overnight. Enclosed branches contained 8 to 12 leaves  
127 corresponding to a range of 1.4 to 3.6 g of dry matter and 110 to 320 cm<sup>2</sup> of leaf surface, respectively.

## 128 2.3 Ecophysiological parameters

129 Exchange of CO<sub>2</sub> and H<sub>2</sub>O from the enclosed branches was continuously (every min) measured using infrared gas  
130 analysers (IRGA 840A®, LI-COR) concomitantly with BVOCs emission measurements (cf. 2.4). Gas exchange  
131 values were averaged by taking into account all the data measured between 12h and 15h (local time). Net  
132 photosynthesis ( $P_n$ ,  $\mu$ molCO<sub>2</sub> m<sup>-2</sup> s<sup>-1</sup>) and stomatal conductance to water ( $G_w$ , mmolH<sub>2</sub>O m<sup>-2</sup> s<sup>-1</sup>) were calculated  
133 using equations described by Von Caemmerer and Farquhar (1981) as used in Genard-Zielinski *et al.* (2015) (for  
134 more details, see Appendix A, equations A1 to A4). Leaves from enclosed branches were directly collected after  
135 gas exchange sampling to accurately measure leaf surface with a leaf area meter.  $P_n$  and  $G_w$  were hence expressed  
136 in a leaf surface basis. After that, leaves were freeze-dried to assess their dry mass.

## 137 2.4 BVOCs analysis

138 A PTR-ToF-MS 8000 instrument (Ionicon Analytik GmbH, Innsbruck, Austria) was used for online measurements  
139 of BVOCs emitted by the enclosed branches. A multi-position common outlet flow path selector valve system  
140 (Vici) and a vacuum pump were used to sequentially select air samples from: amplified drought, inlet air, natural  
141 drought, ambient air and catalyst. The catalyst consists in a 25 cm long stainless steel tubing, filled with platinum  
142 wool and heated at 350°C to efficiently remove VOCs from sample and measure potential instrumental background  
143 levels. Each sample was analysed every hour, with 15min of analysis. Mass spectra in the range 0-500amu were  
144 recorded at 1min integration time. The reaction chamber pressure was fixed at 2.1mbar, the drift tube voltage at  
145 550V and the drift tube temperature at 313 K corresponding to an electric field strength applied to the drift tube

146 (E) to a buffer gas density (N) ratio of 125Td (1Td =  $10^{-17}$  V cm<sup>2</sup>). A calibration gas standard, consisting of a  
147 mixture of 14 aromatic organic compounds (TO-14A Aromatic Mix, Restek Corporation, Bellefonte, USA,  $100 \pm$   
148 10ppb in Nitrogen), was used to experimentally determine the ion relative transmission efficiency. BVOCs  
149 targeted in this study and their corresponding ions include formaldehyde (m/z 31.018), methanol (m/z 33.033),  
150 acetaldehyde (m/z 45.03), acetone (m/z 59.05), isoprene (m/z 41.038, 69.069) and MACR+MVK+ISOPOOH (m/z  
151 71.049, these three compounds were detected with the same m/z with PTR-MS). The signal corresponding to  
152 protonated VOCs was converted into mixing ratios by using the proton transfer rate constants  $k$  given by Cappellin  
153 *et al.* (2012). Formaldehyde concentrations were calculated according to the method described by Vlasenko *et al.*  
154 (2010) to account for its humidity dependent sensitivity.

155 BVOCs emissions rates (ER) were calculated by considering the BVOCs concentrations in the inlet and outlet air  
156 as follows (equation 1):

$$157 \quad ER = \frac{Q_0 * (C_{out} - C_{in})}{B} \quad (1)$$

158 where  $ER$  was expressed in  $\mu\text{gC g}_{\text{DM}}^{-1} \text{h}^{-1}$ ,  $Q_0$  was the flow rate of the air introduced into the chamber ( $\text{L h}^{-1}$ ),  $C_{out}$   
159 and  $C_{in}$  were the concentrations in the inflowing and outflowing air ( $\mu\text{gC L}^{-1}$ ), respectively, and  $B$  was the total  
160 dry biomass matter ( $\text{g}_{\text{DM}}$ ). Daily cycles were made by averaging measured emissions of all trees every hour.

## 161 2.5 Emission algorithms

162 The light and/or temperature dependence of *Q. pubescens* BVOCs (isoprene and highly volatile compounds) under  
163 natural and amplified drought was tested using both the  $L+T$  and  $T$  algorithms. Emission rates calculated according  
164 to these algorithms (afterwards, called  $ER_{L+T}$  and  $ER_T$ , respectively) were calculated using the equations described  
165 in Guenther *et al.* (1995) (for more details, see Appendix B, equations B1 to B5). The empirical coefficient  $\beta$  (used  
166 in the  $T$  algorithm) was determined for each compound according to the season and the treatment through the slope  
167 of correlation between the natural logarithm of emissions rates (measured emissions,  $\mu\text{gC g}_{\text{DM}}^{-1} \text{h}^{-1}$ ) and  
168 experimental temperature (K). Emissions factors ( $EF$ ), that are emissions rates at standard conditions of light and  
169 temperature,  $1000 \mu\text{mol m}^{-2} \text{s}^{-1}$  and  $30^\circ\text{C}$ , were used to calculate modelled emissions and were determined for each  
170 compound under each season and treatment tree by tree.  $EF$  values correspond to the slope of the correlation  
171 between experimental emission rates and  $C_l * C_t$  when using the  $L+T$  algorithm or  $C_T$  when using the  $T$  algorithm  
172 (without forcing data to pass through the origin, see Appendix B for a full description of  $C_l * C_t$  and  $C_T$ ).  $R^2$  and  $p$ -  
173 value of these correlations tree by tree are presented in tables S1 – S6 (supplementary files) and all parameters  
174 used for the calculation of modelled emissions are presented in tables S7 and S8 (for  $C_l * C_t$  and  $C_T$ , respectively,  
175 in supplementary files).

## 176 2.6 Data treatment

177 Data treatment was performed with the software STATGRAPHICS® centurion XV (Statpoint, Inc). After having  
178 checked the normality of the data set, two-way repeated measures ANOVA were carried out to evaluate the  
179 variability of  $P_n$ ,  $G_w$  and BVOC emission rates according to the drought treatment and season. Correlation  
180 coefficient ( $R^2$ ) and slope (called “sl” afterwards) from Pearson’s correlations between measured and modelled  
181 emissions were used to evaluate the algorithm ( $L+T$  or  $T$ ) that better predicted *Q. pubescens* emissions under the  
182 different drought conditions and seasonal cycle. These correlations indicate if there was an under- or over-

183 estimation of modelled emissions with  $sl < 1$  and  $sl > 1$ , respectively, or if the intercept (called “b” afterwards) are  
184 different from 0. For that, slope comparison tests were performed to check for slope significant differences from  
185 1 and intercept tests were performed to check for intercept significant differences from 0. These correlations were  
186 obtained without forcing data to pass through the origin and with this relation: modelled emissions =  $a \cdot \text{measured}$   
187 emission + b.

### 188 3. Results and discussion

#### 189 3.1 Ecophysiological parameters

190 The physiology of *Q. pubescens* was slightly impacted by amplified drought over the whole study (Fig. 2), with a  
191 decrease of  $G_w$  under amplified drought compared to natural drought – ranging from 44 % in spring ( $P < 0.1$ ) to  
192 55 % in summer ( $P < 0.01$ , Table 1). In autumn, there was no significant difference between both treatments.  $P_n$   
193 was only slightly reduced in summer by 36 % ( $P < 0.1$ ) with no difference for the others season. Thus, the stomatal  
194 closure observed had a slight impact on carbon assimilation. Indeed, *Q. pubescens* has a high stem hydraulic  
195 efficiency (Nardini & Pitt 1999) which compensates stomatal closure since it allows to use water more efficiently,  
196 thus, maintaining  $P_n$ . Moreover, it must be noted that an increase of  $P_n$  was observed in autumn and could likely  
197 be attributed to autumnal rains. These results showed that the amplified drought artificially applied to *Q. pubescens*  
198 at O<sub>3</sub>HP led to a moderate drought for this species, based on a moderate reduction of the physiological  
199 performances (Niinemets 2010).

#### 200 3.2 Effect of drought on BVOCs emissions

201 Emissions of all BVOCs followed during this experimentation were reduced under amplified drought compared  
202 to natural drought, especially in spring and summer (Table 1) except for acetaldehyde emissions. Indeed,  
203 acetaldehyde was not significantly different between both treatments probably due to a large variability of the data  
204 set. In autumn, for all BVOCs, there was no difference between both plots. The decrease of oxygenated BVOCs  
205 in spring and summer under amplified drought (e.g. methanol, MACR+MVK+ISOPOOH, formaldehyde, acetone)  
206 could be explained by stomatal closure in spring and summer under amplified drought since emissions of these  
207 compounds are strongly bound to  $G_w$  (Niinemets *et al.* 2004). Isoprene emissions were also reduced in spring and  
208 summer during the 3<sup>rd</sup> year of this experiment whereas an increase had been observed in the first year (Génard-  
209 Zielinski *et al.* in prep) as well as what had been shown by Brüggemann and Schnitzler (2002) but this work was  
210 conducted with potted plants. The isoprene decrease observed in our experiment cannot be explained by the  
211 stomatal closure because this compound could also be emitted through the cuticle (Sharkey & Yeh 2001). It could  
212 rather be due to the decrease of  $P_n$  which reduced the carbon availability to produce isoprene. Moreover, carbon  
213 assimilated through  $P_n$  can be also invested into the synthesis of other defense compounds leading to a decrease  
214 of isoprene production and emission.

#### 215 3.3 Effect of drought on light and/or temperature dependence through a seasonal cycle

216 All six BVOCs monitored showed daytime light and temperature dependencies (isoprene, degradation products of  
217 isoprene and acetaldehyde), while three BVOCs (methanol, acetone and formaldehyde) also showed emissions  
218 during the night despite the absence of light under constant temperature.

219  
220 Regarding the light and temperature dependencies, the daily cycle of isoprene emissions (Fig. 3) showed that this  
221 compound clearly responds to light and temperature as already known (Guenther *et al.* 1993) and that this response  
222 is not impacted by amplified drought. Isoprene can protect thylakoids from oxidative damage (Velikova *et al.*  
223 2011) occurring mainly during the day which can explain this kind of dependence. Yet, our results show the  
224 intensity of isoprene emission factor under natural and amplified drought is very different independently of the  
225 season. The modelled emissions were roughly very representative of measured emissions. We note, however, that  
226 in spring, under natural drought, emissions were slightly underestimated ( $sl = 0.84$ ,  $P < 0.05$ ,  $R^2 = 0.90$ ). It suggests  
227 that although light and temperature remain the main factors driving isoprene emissions in spring but other  
228 parameters explain 10% of these emissions. At this season, plants likely needed to produce more isoprene to protect  
229 the establishment of photosynthetic machinery in the new leaves which could slightly modify the effects of light  
230 and temperature on isoprene emissions.

231 MACR+MVK+ISOPOOH emissions, as isoprene, seemed to respond better to light and temperature than to only  
232 temperature (Fig. S2 in supplementary files) since correlations between measured emissions and  $ER_{L+T}$  were  
233 always better than correlations with  $ER_T$ . Since MACR+MVK+ISOPOOH are oxidation products of isoprene  
234 (Oikawa & Lerdau 2013), it is not surprising that these compounds followed the same pattern than isoprene in  
235 terms of dependence to light and temperature. The estimations of  $ER_{L+T}$  were quite good except in spring under  
236 natural drought where a slight underestimation was observed ( $sl = 0.87$ ,  $P < 0.05$ ). This underestimation can be  
237 explain by the underestimation of isoprene emissions observed at the same time since MACR+MVK+ISOPOOH  
238 comes from isoprene oxidation.

239 The dependence of acetaldehyde emissions to light and/or temperature is very contrasted; studies have shown that  
240 they are bound to both light and temperature (Jardine 2008; Fares *et al.* 2011) or to temperature only (Hayward *et*  
241 *al.* 2004). Our results suggested that acetaldehyde emissions were mainly bound to light and temperature (Fig. 4).  
242 Indeed, correlations between measured and  $ER_{L+T}$  were always better than with  $ER_T$ . However, some discrepancies  
243 were observed. Under natural drought, underestimations were observed in spring and summer ( $sl = 0.72$ , and  $sl =$   
244  $0.57$ ,  $P < 0.05$ , respectively) whereas in autumn, there was a good estimation ( $sl = 0.86$ ,  $P > 0.05$ ). Under amplified  
245 drought, underestimation was only observed in summer ( $sl = 0.80$ ,  $P < 0.05$ ). Trees studied in this experiment did  
246 not show the same dependence to light and temperature for acetaldehyde emissions.  $R^2$  of the correlation  
247 determining EF (performed tree by tree), varies from 0.34 to 0.90 in summer, from 0.67 to 0.92 in spring, under  
248 natural drought. Under amplified drought,  $R^2$  varies from 0.22 to 0.83 in summer (Tables S6 in supplementary  
249 files). These results suggest that the effect of light and temperature on acetaldehyde emissions strongly depend on  
250 tree considered and could explain the underestimations observed in our experiment. Moreover, daily cycles of  
251 acetaldehyde emissions presented also an emissions burst in the morning (at 7h, local time) in spring (under both  
252 treatments) and in summer (only under natural drought). Acetaldehyde can be produced due to an overflow of  
253 pyruvic acid during light-dark transitions. Cytosolic pyruvic acid levels rise rapidly and it can be converted into  
254 acetaldehyde by pyruvate decarboxylase (Fall 2003). This mechanism could explain the morning burst for this  
255 compound and the fact that no emissions during the night was observed.

256

257 We observed emissions of methanol, acetone and formaldehyde during the night under no light and constant  
258 temperature (around 20°C, see supplementary files S1). Correlations between  $ER_{L+T}$  or  $ER_T$  and measured  
259 methanol emissions were very similar especially in spring and summer (Fig. 5). However, some observed  
260 phenomena suggested that methanol emission was sustained by temperature in the absence of light. Indeed, the  
261 burst in the early morning (at 7h, local time), similar to acetaldehyde, was observed when stomata opened in spring  
262 and summer, independently of the drought treatment although it was clearer under natural than amplified drought.  
263 This burst can be explained by a strong release of this compound that has been accumulated in the intercellular air  
264 space and leaf liquid pools (due to the relative high polarity of methanol) at night when stomata are closed (Hüve  
265 *et al.* 2007). Moreover, for both drought treatments, methanol emissions during the night were observed at any  
266 seasons (especially autumn) which could be explained by nocturnal temperatures (roughly constant) that sufficed  
267 to maintain the biochemical processes involved in methanol formation. Methanol emissions, which result from the  
268 demethylation of pectin during the leaf elongation, has already been described to be temperature dependent alone  
269 (Hayward *et al.* 2004; Folkers *et al.* 2008). However, our results suggest that methanol emissions respond strongly  
270 to light and temperature during the day. This kind of diurnal emissions cycle has already been described by Smiatek  
271 and Steinbrecher (2006). Our results about daily cycles of acetone emissions (Fig. S3 in supplementary files)  
272 showed that this compound responded better to light and temperature than only temperature since correlations  
273 were better with  $ER_{L+T}$ . Under natural drought, the modelled emissions were well representative of measured  
274 emissions in summer. By contrast, in spring and in autumn, slight underestimations were observed ( $sl = 0.88$ ,  $P <$   
275  $0.05$  and  $sl = 0.69$ ,  $P < 0.05$ , respectively). Under amplified drought, good estimations were observed in summer  
276 and autumn but in spring, there was an overestimation of modelled emissions ( $sl = 1.27$ ,  $P < 0.05$ ). Previous studies  
277 have shown that acetone rather depends on temperature alone (Fares *et al.* 2011) or to light and temperature (Jacob  
278 *et al.* 2002), indicating that its dependence on light and/or temperature remains unclear. During the day, acetone  
279 emissions were dependent on light and temperature and emissions still occurred during the night, especially in  
280 autumn. Alike methanol, nocturnal temperatures could allow to maintain acetone formation (Smiatek &  
281 Steinbrecher 2006). Acetone is a by-product of plant metabolism (Jacob *et al.* 2002) and its production can be  
282 enzymatic and non-enzymatic (Fall 2003) which can explain these observed differences through the day. We can  
283 suppose that acetone emissions observed during the day could come from the enzymatic activity and, on the  
284 contrary, during the night, they could come from the non-enzymatic production.

285 Formaldehyde emissions followed the same pattern than methanol and acetone emissions (Fig. S4 in  
286 supplementary files), especially in autumn. By considering only the daytime (correlation with  $L+T$  modelled  
287 emissions), there were good estimations in summer and autumn and a slight underestimation was observed in  
288 spring ( $sl = 0.89$ ,  $P < 0.05$ ) for natural drought. Under amplified drought, correlations indicated that  $L+T$  modelled  
289 emissions were well representative of measured emissions, but some negative emissions were observed in summer  
290 which suggested a deposition or an uptake of this compound by leaves as already highlighted by Seco *et al.* (2008).  
291 This phenomenon could have a role in stress tolerance, since formaldehyde can be catabolised (mainly through  
292 oxidations) within leaves leading to  $CO_2$  formation (Oikawa & Lerdau 2013). Emissions during the night suggest  
293 that formaldehyde came from another source than oxidation within leaves since oxidations occur mainly during  
294 the day due to an excess of light in chloroplasts, principal place of reactive oxygen species production (Asada  
295 2006). Thus, formaldehyde emissions observed during the night could result from, for example, the glyoxylate



296 decarboxylation or the dissociation of 5,10-methylene-THF (Oikawa & Lerdau 2013). Predicting emissions rates  
297 of these 3 compounds (methanol, acetone and formaldehyde), during the night, seem to require other parameters  
298 such as a temperature threshold, below which methanol, acetone and formaldehyde synthesis and so emissions do  
299 not occur.

#### 300 **4 Conclusion**

301 After 3 years of amplified drought, all BVOC emissions were reduced in spring and summer compared to natural  
302 drought whereas, in autumn, an increase was observed for some compounds. These results are in opposition with  
303 the results obtained after only one year of amplified drought (2012), especially for isoprene, where an increase  
304 was observed for this compound (Génard-Zielinski *et al.* in prep). Amplified drought did not seem to shift the  
305 dependence to light and/or temperature which remained unchanged between treatments.  
306 Moreover, two different dependence behaviours were found: (i) all six BVOCs monitored showed daytime light  
307 and temperature dependencies while (ii) only three BVOCs (methanol, acetone and formaldehyde) also showed  
308 that their emissions were maintained during the night with no light at rather constant nocturnal temperatures.  
309 Moreover, some phenomena, such as methanol and acetaldehyde emissions bursts in early morning or the  
310 formaldehyde deposition/uptake (formaldehyde), were not assessed by either  $L+T$  or  $T$  algorithm.

#### 311 **Appendix A: calculation of ecophysiological parameters**

312 Net photosynthesis ( $P_n$ ,  $\mu\text{molCO}_2 \text{ m}^{-2} \text{ s}^{-1}$ ) was calculated using equations described by Von Caemmerer and  
313 Farquhar (1981) as follows:

$$314 \quad P_n = \frac{F*(Cr-Cs)}{S} - CS * E \quad (A1)$$

315 Where  $F$  is the inlet air flow ( $\text{mol s}^{-1}$ ),  $C_s$  and  $C_r$  are the sample and reference  $\text{CO}_2$  molar fraction respectively  
316 (ppm),  $S$  is the leaf surface ( $\text{m}^2$ ),  $C_s * E$  is the fraction of  $\text{CO}_2$  diluted in water evapotranspiration and  $E$  ( $\text{molH}_2\text{O}$   
317  $\text{m}^{-2} \text{ s}^{-1}$  then transformed in  $\text{mmolH}_2\text{O m}^{-2} \text{ s}^{-1}$ , afterward) is the transpiration rate calculated as follow:

$$318 \quad E = \frac{F*(Ws-Wr)}{S*(1-Ws)} \quad (A2)$$

319 where  $W_s$  and  $W_r$  are the sample and the reference  $\text{H}_2\text{O}$  molar fraction respectively ( $\text{molH}_2\text{O mol}^{-1}$ ).

320 Stomatal conductance to water ( $G_w$ ,  $\text{molH}_2\text{O m}^{-2} \text{ s}^{-1}$  then transformed in  $\text{mmolH}_2\text{O m}^{-2} \text{ s}^{-1}$ ) was calculated using  
321 the following equation:

$$322 \quad G_w = \frac{E*(1-\frac{Wl-Ws}{2})}{Wl-Ws} \quad (A3)$$

323 where  $W_l$  is the molar concentration of water vapour within the leaf ( $\text{molH}_2\text{O mol}^{-1}$ ) calculated as follows:

$$324 \quad W_l = \frac{V_{psat}}{P} \quad (A4)$$

325 where  $V_{psat}$  is the saturated vapour pressure (kPa) and  $P$  was the atmospheric pressure (kPa).

#### 326 **Appendix B: Modelled emissions calculation**

327 The modelled emissions rates according to light and temperature ( $ER_{L+T}$ ) or the temperature algorithm ( $ER_T$ ) were  
328 calculated according to algorithms described in Guenther *et al.* (1995) as follows :

$$329 \quad ER_{L+T} = EF_{L+T} * C_l * C_t \quad (B1)$$

330 where  $EF_{L+T}$  is the emission factor at 1000  $\mu\text{mol m}^{-2} \text{s}^{-1}$  of photosynthetically active radiation (PAR) and 30°C of  
331 temperature (obtained with the slope of the correlation between experimental emissions and  $C_l * C_t$  without forcing  
332 data to pass through the origin),  $C_l$  and  $C_t$  correspond to light and temperature dependence factors respectively and  
333 were calculated with the following formulae:

$$334 \quad C_l = \frac{\alpha C_{L1} L}{\sqrt{1 + \alpha^2 L}} \quad (B2)$$

$$335 \quad C_t = \frac{\exp\left(\frac{C_{T1}(T - T_S)}{RT_S T}\right)}{1 + \exp\left(\frac{C_{T2}(T - T_M)}{RT_S T}\right)} \quad (B3)$$

336 where  $\alpha = 0.0027$ ,  $C_{L1} = 1.066$ ,  $C_{T1} = 95000 \text{J mol}^{-1}$ ,  $C_{T2} = 230000 \text{J mol}^{-1}$ ,  $T_M = 314 \text{K}$  are empirically derived  
337 constants,  $L$  is the photosynthetically active radiation (PAR) flux ( $\mu\text{mol m}^{-2} \text{s}^{-1}$ ),  $T$  is the leaf experimental  
338 temperature (K) and  $T_S$  is the leaf temperature at standard condition (303K).

339 Modelled emissions according to temperature alone that is  $ER_T$ , was calculated as follows:

$$340 \quad ER_T = EF_T * C_T \quad (B4)$$

341 where  $EF_T$  is the emission factor at 30°C of temperature (obtained with the slope of the correlation between  
342 experimental emissions and  $C_T$  without forcing data to pass through the origin) and  $C_T$  is a temperature dependence  
343 factor calculated as follows:

$$344 \quad C_T = \exp[\beta(T - T_S)] \quad (B5)$$

345 where  $\beta$  is an empirical coefficient (with a standard variation value of  $0.09 \text{K}^{-1}$  used in literature when not measured)  
346 determined, in this study, for each compound according to the season and the treatment through the slope of the  
347 correlation between the natural logarithm of measured emissions rates ( $ER$ ,  $\mu\text{gC g}_{\text{DM}}^{-1} \text{h}^{-1}$ ) and experimental  
348 temperature (expressed in K),  $T$  is the leaf experimental temperature (K) and  $T_S$  is the standard temperature (303K).

#### 349 **Author contribution**

350 AS, EO and CF designed the research and the experimental design. AS, BTR, EO and CF conducted the research.  
351 AS, CB, BTR, and CL collected and analyzed the data. AS, EO, CB, HW, BTR, AA and CF wrote the manuscript

#### 352 **Competing interests**

353 The authors declare that they have no conflict of interest.

#### 354 **Acknowledgments**

355 This work was supported by the French National Agency for Research (ANR) through the SecPriMe<sup>2</sup> project  
356 (ANR-12-BSV7-0016-01); Europe (FEDER) and ADEME/PACA for PhD funding. We are grateful to FR3098  
357 ECCOREV for the O<sub>3</sub>HP facilities (<https://o3hp.obs-hp.fr/index.php/fr/>). We are very grateful to J.-P. Orts, I.  
358 Reiter. We also thank all members of the DFME team from IMBE and particularly: S. Greff, S. Dupouyet and A.  
359 Bousquet-Melou for their help during measurements and analysis. We thank also, the Université Paris Diderot-

360 Paris7 for its support. The authors thank the MASSALYA instrumental platform (Aix Marseille Université,  
361 ice.univ-amu.fr) for the analysis and measurements used in this publication.

## 362 References

- 363 Arneth A., Monson R., Schurgers G., Niinemets Ü. & Palmer P. (2008). Why are estimates of global terrestrial  
364 isoprene emissions so similar (and why is this not so for monoterpenes)? *Atmospheric Chemistry and*  
365 *Physics*, 8, 4605-4620.
- 366 Asada K. (2006). Production and scavenging of reactive oxygen species in chloroplasts and their functions. *Plant*  
367 *physiology*, 141, 391-396.
- 368 Beauchamp J., Wisthaler A., Hansel A., Kleist E., Miebach M., NIINEMETS Ü., Schurr U. & WILDT J. (2005).  
369 Ozone induced emissions of biogenic VOC from tobacco: relationships between ozone uptake and  
370 emission of LOX products. *Plant, Cell & Environment*, 28, 1334-1343.
- 371 Brüggemann N. & Schnitzler J.P. (2002). Comparison of Isoprene Emission, Intercellular Isoprene  
372 Concentration and Photosynthetic Performance in Water-Limited Oak (*Quercus pubescens* Willd. and  
373 *Quercus robur* L.) Saplings. *Plant Biology*, 4, 456-463.
- 374 Cappellin L., Karl T., Probst M., Ismailova O., Winkler P.M., Soukoulis C., Aprea E., Märk T.D., Gasperi F. &  
375 Biasioli F. (2012). On quantitative determination of volatile organic compound concentrations using  
376 proton transfer reaction time-of-flight mass spectrometry. *Environmental science & technology*, 46,  
377 2283-2290.
- 378 Dindorf T., Kuhn U., Ganzeveld L., Schebeske G., Ciccioli P., Holzke C., Köble R., Seufert G. & Kesselmeier J.  
379 (2006). Significant light and temperature dependent monoterpene emissions from European beech  
380 (*Fagus sylvatica* L.) and their potential impact on the European volatile organic compound budget.  
381 *Journal of Geophysical Research: Atmospheres*, 111.
- 382 Fall R. (2003). Abundant oxygenates in the atmosphere: a biochemical perspective. *Chemical reviews*, 103,  
383 4941-4952.
- 384 Fares S., Gentner D.R., Park J.-H., Ormeno E., Karlik J. & Goldstein A.H. (2011). Biogenic emissions from  
385 *Citrus* species in California. *Atmospheric Environment*, 45, 4557-4568.
- 386 Folkers A., Hüve K., Ammann C., Dindorf T., Kesselmeier J., Kleist E., Kuhn U., Uerlings R. & Wildt J. (2008).  
387 Methanol emissions from deciduous tree species: dependence on temperature and light intensity. *Plant*  
388 *biology*, 10, 65-75.
- 389 Fortunati A., Barta C., Brilli F., Centritto M., Zimmer I., Schnitzler J.P. & Loreto F. (2008). Isoprene emission is  
390 not temperature - dependent during and after severe drought - stress: a physiological and biochemical  
391 analysis. *The Plant Journal*, 55, 687-697.
- 392 Funk J., Mak J. & Lerda M. (2004). Stress - induced changes in carbon sources for isoprene production in  
393 *Populus deltoides*. *Plant, Cell & Environment*, 27, 747-755.
- 394 Genard-Zielinski A.-C., Boissard C., Fernandez C., Kalogridis C., Lathière J., Gros V., Bonnaire N. & Ormeño  
395 E. (2015). Variability of BVOC emissions from a Mediterranean mixed forest in southern France with a  
396 focus on *Quercus pubescens*. *Atmospheric Chemistry and Physics Discussions*, 14, 17225-17261.
- 397 Giorgi F. & Lionello P. (2008). Climate change projections for the Mediterranean region. *Global and Planetary*  
398 *Change*, 63, 90-104.
- 399 Guenther A., Hewitt C.N., Erickson D., Fall R., Geron C., Graedel T., Harley P., Klinger L., Lerda M., McKay  
400 W.A., Pierce T., Scholes B., Steinbrecher R., Tallamraju R., Taylor J. & Zimmerman P. (1995). A  
401 global model of natural volatile organic compound emissions. *Journal of Geophysical Research:*  
402 *Atmospheres*, 100, 8873-8892.
- 403 Guenther A., Jiang X., Heald C., Sakulyanontvittaya T., Duhl T., Emmons L. & Wang X. (2012). The Model of  
404 Emissions of Gases and Aerosols from Nature version 2.1 (MEGAN2. 1): an extended and updated  
405 framework for modeling biogenic emissions.
- 406 Guenther A., Karl T., Harley P., Wiedinmyer C., Palmer P. & Geron C. (2006). Estimates of global terrestrial  
407 isoprene emissions using MEGAN (Model of Emissions of Gases and Aerosols from Nature).  
408 *Atmospheric Chemistry and Physics*, 6, 3181-3210.
- 409 Guenther A.B., Zimmerman P.R., Harley P.C., Monson R.K. & Fall R. (1993). Isoprene and monoterpene  
410 emission rate variability: model evaluations and sensitivity analyses. *Journal of Geophysical Research:*  
411 *Atmospheres* (1984-2012), 98, 12609-12617.
- 412 Hallquist M., Wenger J., Baltensperger U., Rudich Y., Simpson D., Claeys M., Dommen J., Donahue N., George  
413 C. & Goldstein A. (2009). The formation, properties and impact of secondary organic aerosol: current  
414 and emerging issues. *Atmospheric Chemistry and Physics*, 9, 5155-5236.

415 Harrison S.P., Morfopoulos C., Dani K., Prentice I.C., Arneth A., Atwell B.J., Barkley M.P., Leishman M.R.,  
416 Loreto F. & Medlyn B.E. (2013). Volatile isoprenoid emissions from plastid to planet. *New Phytol.*,  
417 197, 49-57.

418 Hayward S., Tani A., Owen S.M. & Hewitt C.N. (2004). Online analysis of volatile organic compound emissions  
419 from Sitka spruce (*Picea sitchensis*). *Tree Physiology*, 24, 721-728.

420 Heikes B.G., Chang W., Pilson M.E., Swift E., Singh H.B., Guenther A., Jacob D.J., Field B.D., Fall R. &  
421 Riemer D. (2002). Atmospheric methanol budget and ocean implication. *Global Biogeochemical*  
422 *Cycles*, 16, 80-1-80-13.

423 Hüve K., Christ M., Kleist E., Uerlings R., Niinemets Ü., Walter A. & Wildt J. (2007). Simultaneous growth and  
424 emission measurements demonstrate an interactive control of methanol release by leaf expansion and  
425 stomata. *Journal of experimental botany*, 58, 1783-1793.

426 IPCC (2013). In: *Contribution of working group I to the fifth assessment report of the intergovernmental panel on*  
427 *climate change*. Cambridge University Press Cambridge.

428 Jacob D.J., Field B.D., Jin E.M., Bey I., Li Q., Logan J.A., Yantosca R.M. & Singh H.B. (2002). Atmospheric  
429 budget of acetone. *Journal of Geophysical Research: Atmospheres (1984–2012)*, 107, ACH 5-1-ACH  
430 5-17.

431 Jardine J. (2008). Plant physiological and environmental controls over the exchange of acetaldehyde between  
432 forest canopies and the atmosphere. *Biogeosciences*, 5.

433 Jimenez J., Canagaratna M., Donahue N., Prevot A., Zhang Q., Kroll J.H., DeCarlo P.F., Allan J.D., Coe H. &  
434 Ng N. (2009). Evolution of organic aerosols in the atmosphere. *Science*, 326, 1525-1529.

435 Keenan T., Niinemets Ü., Sabate S., Gracia C. & Peñuelas J. (2009). Process based inventory of isoprenoid  
436 emissions from European forests: model comparisons, current knowledge and uncertainties.  
437 *Atmospheric Chemistry and Physics Discussions*, 9, 6147-6206.

438 Kesselmeier J. & Staudt M. (1999). Biogenic volatile organic compounds (VOC): an overview on emission,  
439 physiology and ecology. *Journal of Atmospheric Chemistry*, 33, 23-88.

440 Lippmann M. (1989). Health effects of ozone a critical review. *Japca*, 39, 672-695.

441 Liu Y., Siekmann F., Renard P., El Zein A., Salque G., El Haddad I., Temime-Roussel B., Voisin D., Thissen R.  
442 & Monod A. (2012). Oligomer and SOA formation through aqueous phase photooxidation of  
443 methacrolein and methyl vinyl ketone. *Atmospheric Environment*, 49, 123-129.

444 Menut L., Bessagnet B., Khvorostyanov D., Beekmann M., Blond N., Colette A., Coll I., Curci G., Foret G. &  
445 Hodzic A. (2014). CHIMERE 2013: a model for regional atmospheric composition modelling.  
446 *Geoscientific Model Development*, 6, 981-1028.

447 Millet D.B., Guenther A., Siegel D.A., Nelson N.B., Singh H.B., de Gouw J.A., Warneke C., Williams J.,  
448 Eerdekens G. & Sinha V. (2010). Global atmospheric budget of acetaldehyde: 3-D model analysis and  
449 constraints from in-situ and satellite observations. *Atmospheric Chemistry and Physics*, 10, 3405-3425.

450 Monson R.K., Trahan N., Rosenstiel T.N., Veres P., Moore D., Wilkinson M., Norby R.J., Volder A., Tjoelker  
451 M.G. & Briske D.D. (2007). Isoprene emission from terrestrial ecosystems in response to global  
452 change: minding the gap between models and observations. *Philosophical Transactions of the Royal*  
453 *Society of London A: Mathematical, Physical and Engineering Sciences*, 365, 1677-1695.

454 Nardini A. & Pitt F. (1999). Drought resistance of *Quercus pubescens* as a function of root hydraulic  
455 conductance, xylem embolism and hydraulic architecture. *New Phytol.*, 143, 485-493.

456 Niinemets Ü. (2010). Mild versus severe stress and BVOCs: thresholds, priming and consequences. *Trends in*  
457 *plant science*, 15, 145-153.

458 Niinemets Ü., Loreto F. & Reichstein M. (2004). Physiological and physicochemical controls on foliar volatile  
459 organic compound emissions. *Trends in plant science*, 9, 180-186.

460 Oikawa P.Y. & Lerdau M.T. (2013). Catabolism of volatile organic compounds influences plant survival. *Trends*  
461 *in plant science*, 18, 695-703.

462 Ormeno E., Goldstein A. & Niinemets Ü. (2011). Extracting and trapping biogenic volatile organic compounds  
463 stored in plant species. *TrAC Trends in Analytical Chemistry*, 30, 978-989.

464 Owen S., Harley P., Guenther A. & Hewitt C. (2002). Light dependency of VOC emissions from selected  
465 Mediterranean plant species. *Atmospheric environment*, 36, 3147-3159.

466 Papiez M.R., Potosnak M.J., Goliff W.S., Guenther A.B., Matsunaga S.N. & Stockwell W.R. (2009). The  
467 impacts of reactive terpene emissions from plants on air quality in Las Vegas, Nevada. *Atmospheric*  
468 *Environment*, 43, 4109-4123.

469 Polade S.D., Pierce D.W., Cayan D.R., Gershunov A. & Dettinger M.D. (2014). The key role of dry days in  
470 changing regional climate and precipitation regimes. *Scientific reports*, 4.

471 Pollmann J., Ortega J. & Helmig D. (2005). Analysis of atmospheric sesquiterpenes: Sampling losses and  
472 mitigation of ozone interferences. *Environmental science & technology*, 39, 9620-9629.

473 Quézel P. & Médail F. (2003). *Ecologie et biogéographie des forêts du bassin méditerranéen*. Elsevier Paris.

- 474 Reig-Armiñana J., Calatayud V., Cerveró J., Garcia-Breijo F., Ibars A. & Sanz M. (2004). Effects of ozone on  
475 the foliar histology of the mastic plant (*Pistacia lentiscus* L.). *Environmental Pollution*, 132, 321-331.
- 476 Rinne H., Guenther A., Greenberg J. & Harley P. (2002). Isoprene and monoterpene fluxes measured above  
477 Amazonian rainforest and their dependence on light and temperature. *Atmospheric Environment*, 36,  
478 2421-2426.
- 479 Seco R., Penuelas J. & Filella I. (2008). Formaldehyde emission and uptake by Mediterranean trees *Quercus ilex*  
480 and *Pinus halepensis*. *Atmospheric Environment*, 42, 7907-7914.
- 481 Sharkey T.D. & Yeh S. (2001). Isoprene emission from plants. *Annual review of plant biology*, 52, 407-436.
- 482 Singh H., Chen Y., Tabazadeh A., Fukui Y., Bey I., Yantosca R., Jacob D., Arnold F., Wohlfrom K. & Atlas E.  
483 (2000). Distribution and fate of selected oxygenated organic species in the troposphere and lower  
484 stratosphere over the Atlantic. *Journal of Geophysical Research: Atmospheres (1984–2012)*, 105, 3795-  
485 3805.
- 486 Smiatek G. & Steinbrecher R. (2006). Temporal and spatial variation of forest VOC emissions in Germany in the  
487 decade 1994–2003. *Atmospheric Environment*, 40, 166-177.
- 488 Velikova V., Várkonyi Z., Szabó M., Maslenkova L., Noguez I., Kovács L., Peeva V., Busheva M., Garab G. &  
489 Sharkey T.D. (2011). Increased thermostability of thylakoid membranes in isoprene-emitting leaves  
490 probed with three biophysical techniques. *Plant Physiology*, 157, 905-916.
- 491 Vlasenko A., Macdonald A., Sjostedt S. & Abbatt J. (2010). Formaldehyde measurements by Proton transfer  
492 reaction–Mass Spectrometry (PTR-MS): correction for humidity effects. *Atmospheric Measurement*  
493 *Techniques*, 3, 1055-1062.
- 494 Von Caemmerer S.v. & Farquhar G. (1981). Some relationships between the biochemistry of photosynthesis and  
495 the gas exchange of leaves. *Planta*, 153, 376-387.
- 496 Xie X., Shao M., Liu Y., Lu S., Chang C.-C. & Chen Z.-M. (2008). Estimate of initial isoprene contribution to  
497 ozone formation potential in Beijing, China. *Atmospheric Environment*, 42, 6000-6010.

498

499

500

501

502

503

504

505

506

507

508

509

510

511

512

513

514

515

516

517

518

519 **Table:**

520 **Table 1:** Net photosynthesis ( $P_n$ ,  $\mu\text{molCO}_2 \text{ m}^{-2} \text{ s}^{-1}$ ), stomatal conductance to water ( $G_w$ ,  $\text{mmolH}_2\text{O m}^{-2} \text{ s}^{-1}$ ) and emission rates ( $\mu\text{gC g}_{\text{DM}}^{-1} \text{ h}^{-1}$ ) according to treatment and season.

521 Values represent an average of all data measured between 12h and 15h (local time). Letters denote the difference between drought treatments with a > b and values showed

522 represent the mean  $\pm$  SE, n=5. ND: natural drought and AD: amplified drought with ns = non-significant, (\*) =  $0.05 < P < 0.1$ , \* =  $0.01 < P < 0.05$ , \*\* =  $0.001 < P < 0.01$ ,

Season	Spring			Summer			Autumn			
	Treatments	ND	AD	P	ND	AD	P	ND	AD	P
<b>Pn</b>		11 $\pm$ 1 a	9 $\pm$ 2 a	ns	14 $\pm$ 2 a	9 $\pm$ 1.2 b	(*)	7 $\pm$ 1 a	9 $\pm$ 1 a	ns
<b>Gw</b>		110 $\pm$ 19 a	57 $\pm$ 13 b	(*)	285 $\pm$ 38 a	126 $\pm$ 17 b	**	122 $\pm$ 23 a	74 $\pm$ 21 a	ns
<b>Isoprene</b>		20 $\pm$ 4 a	10 $\pm$ 2 b	*	124 $\pm$ 10 a	81 $\pm$ 11 b	*	3 $\pm$ 1 a	5 $\pm$ 2 a	ns
<b>MACR+MVK+ISOPOOH</b>		0.1 $\pm$ 0.03a	0.1 $\pm$ 0.01 a	ns	0.4 $\pm$ 0.1 a	0.2 $\pm$ 0.02 b	*	0.04 $\pm$ 0.01 a	0.1 $\pm$ 0.01 a	ns
<b>Methanol</b>		1 $\pm$ 0.1 a	0.5 $\pm$ 0.04 b	*	1 $\pm$ 0.2 a	0.6 $\pm$ 0.03 b	*	0.2 $\pm$ 0.03 a	0.2 $\pm$ 0.1 a	ns
<b>Acetaldehyde</b>		1 $\pm$ 0.4 a	1 $\pm$ 0.3 a	ns	2 $\pm$ 0.5 a	1 $\pm$ 0.1 a	ns	1 $\pm$ 0.3 a	1 $\pm$ 0.3 a	ns
<b>Acetone</b>		0.5 $\pm$ 0.1 a	0.2 $\pm$ 0.02 a	ns	1 $\pm$ 0.2 a	0.5 $\pm$ 0.04 b	**	0.4 $\pm$ 0.1 a	0.4 $\pm$ 0.1 a	ns
<b>Formaldehyde</b>		0.2 $\pm$ 0.05 a	0.1 $\pm$ 0.01 a	ns	0.4 $\pm$ 0.1 a	0.1 $\pm$ 0.02 b	**	0.2 $\pm$ 0.1 a	0.3 $\pm$ 0.1 a	ns

523

524 **Figure legends**

525 **Figure 1:** Ombrothermic diagram for natural and amplified drought in 2012, 2013 and 2014. Bars represent mean  
526 monthly precipitation (mm) and curves represent mean monthly temperature (°C). On each amplified drought  
527 graph, the percentage represents the proportion of excluded rain compared to the natural drought plot.

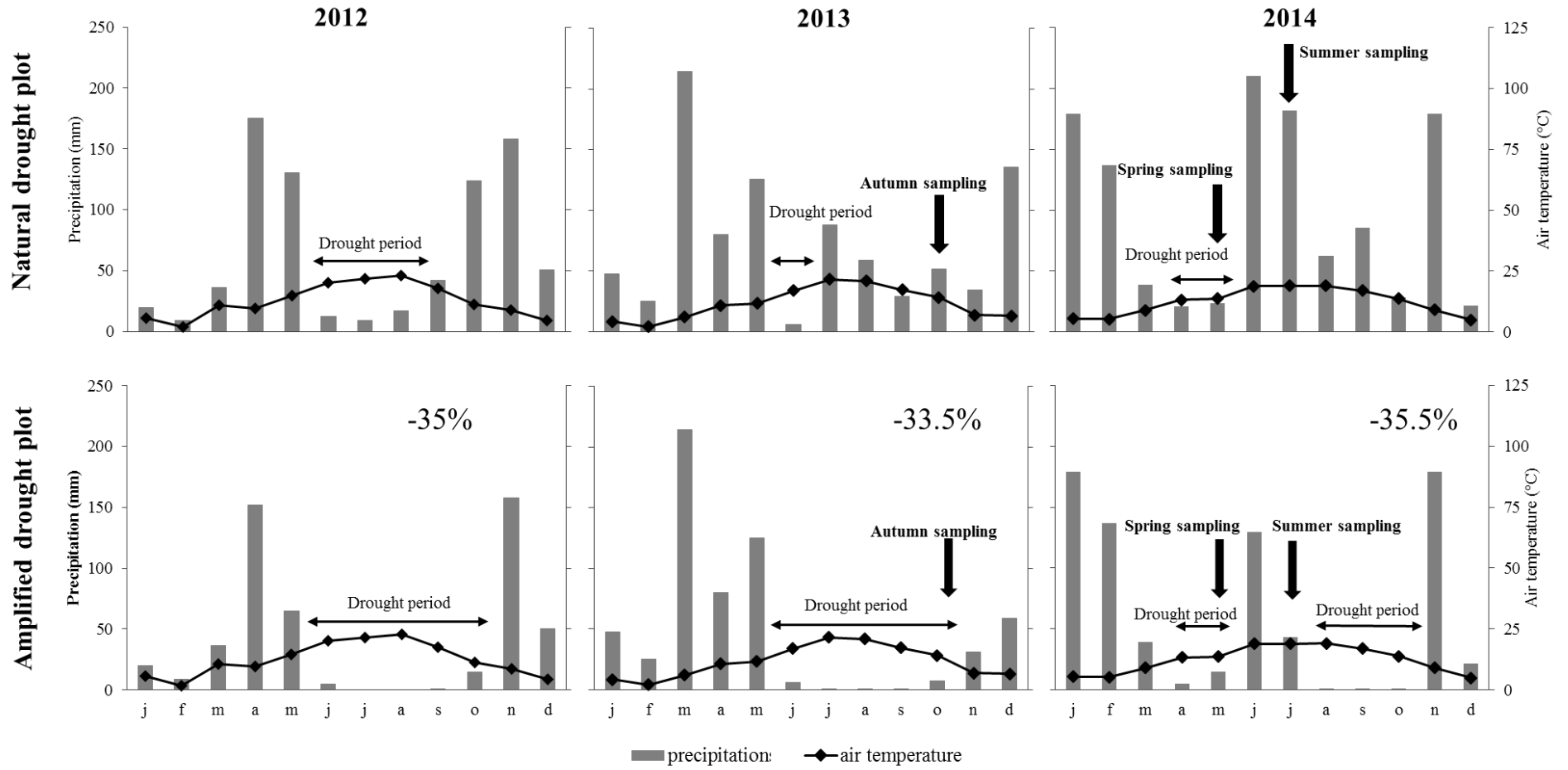
528  
529 **Figure 2:** Diurnal pattern of stomatal conductance ( $G_w$ ) and net photosynthesis ( $P_n$ ) according to drought  
530 treatment and season. Values showed represent means  $\pm$  SE, n=5.

531  
532 **Figure 3:** Diurnal pattern of isoprene emissions rates, where points represent measured emission and the yellow  
533 line corresponds to modelled emissions rates according to the  $L+T$  algorithm ( $ER_{L+T}$ ).  $R^2$  and slope (sl) of  
534 correlations between measured (x axis) and modelled (y axis) emissions are presented in the yellow frame.  
535 Correlations were obtained without forcing data to pass through the origin. Values are mean  $\pm$  SE, n=5.

536  
537 **Figure 4:** Diurnal pattern of acetaldehyde emissions rates, where points represent measured emission, the yellow  
538 line corresponds to modelled emissions rates according to the  $L+T$  algorithm ( $ER_{L+T}$ ) and the dotted line  
539 corresponds to modelled emissions rates according to the  $T$  algorithm ( $ER_T$ ).  $R^2$  and slope (sl) of correlations  
540 between measured (x axis) and modelled (y axis) emissions are presented in the yellow frame for  $L+T$  and in the  
541 white frame for  $T$ . Correlations were obtained without forcing data to pass through the origin. Values are mean  $\pm$   
542 SE, n=5.

543  
544 **Figure 5:** Diurnal pattern of measured methanol emissions rates. Points represent measured emission, the yellow  
545 line corresponds to modelled emissions rates according to the  $L+T$  algorithm ( $ER_{L+T}$ ) and the dotted line  
546 corresponds to modelled emissions rates according to the  $T$  algorithm ( $ER_T$ ).  $R^2$  and slope (sl) of correlations  
547 between measured (x axis) and modelled (y axis) emissions are presented in the yellow frame for  $L+T$  and in the  
548 white frame for  $T$ . Correlations were obtained without forcing data to pass through the origin. Values are mean  $\pm$   
549 SE, n=5.

550  
551  
552  
553  
554  
555  
556



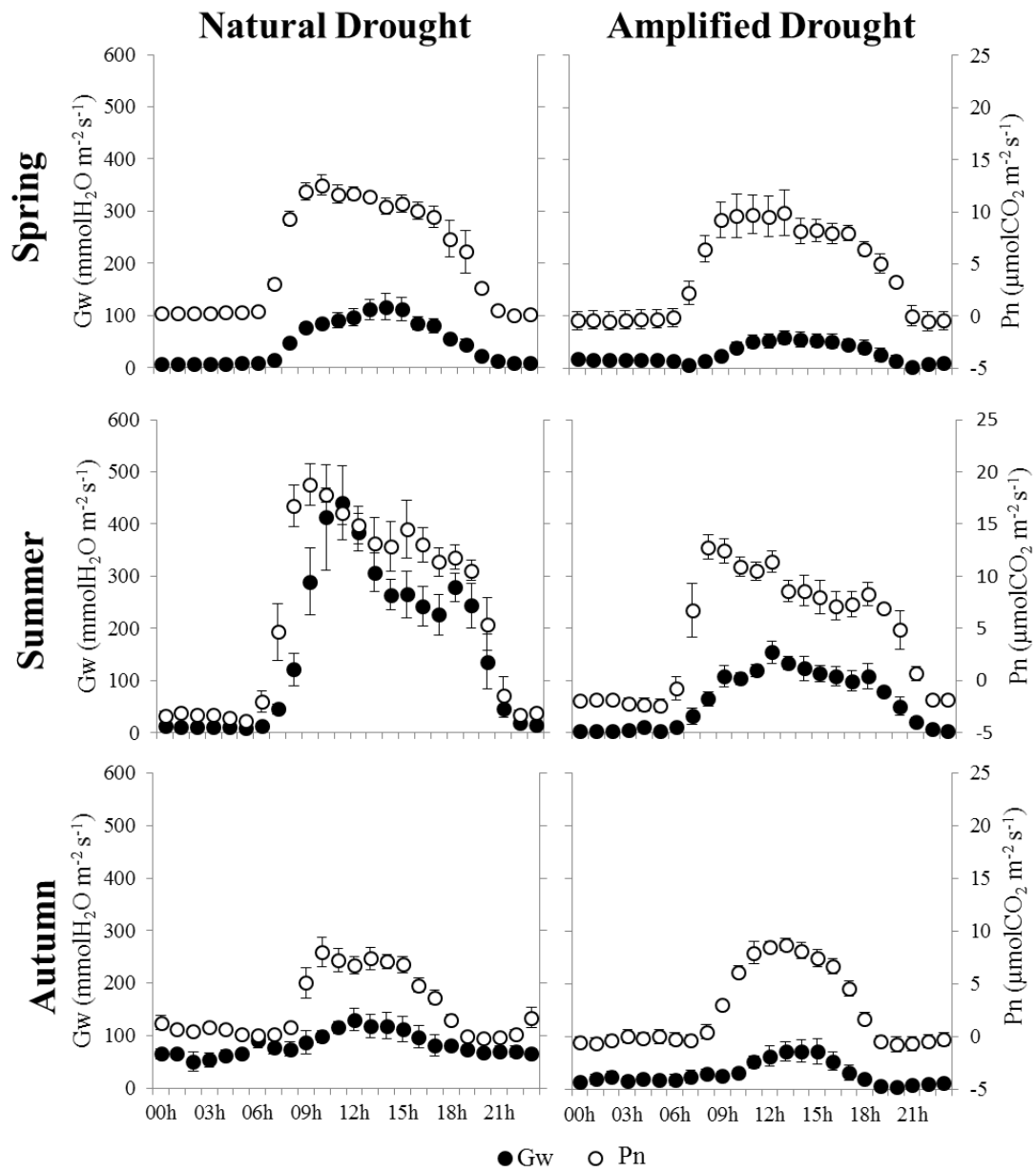
557

558 **Figure 1:**

559

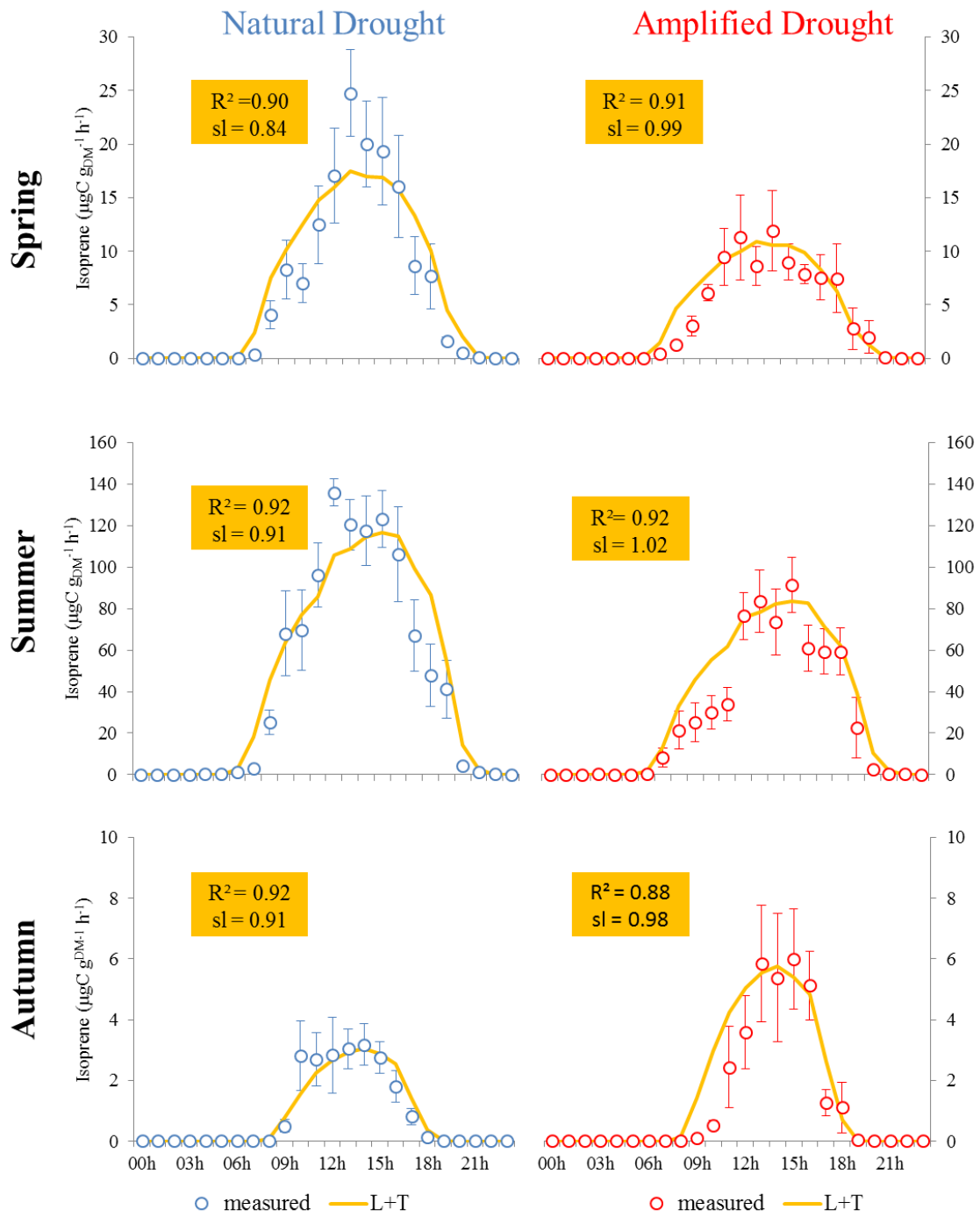
560





562

563 **Figure 2:**

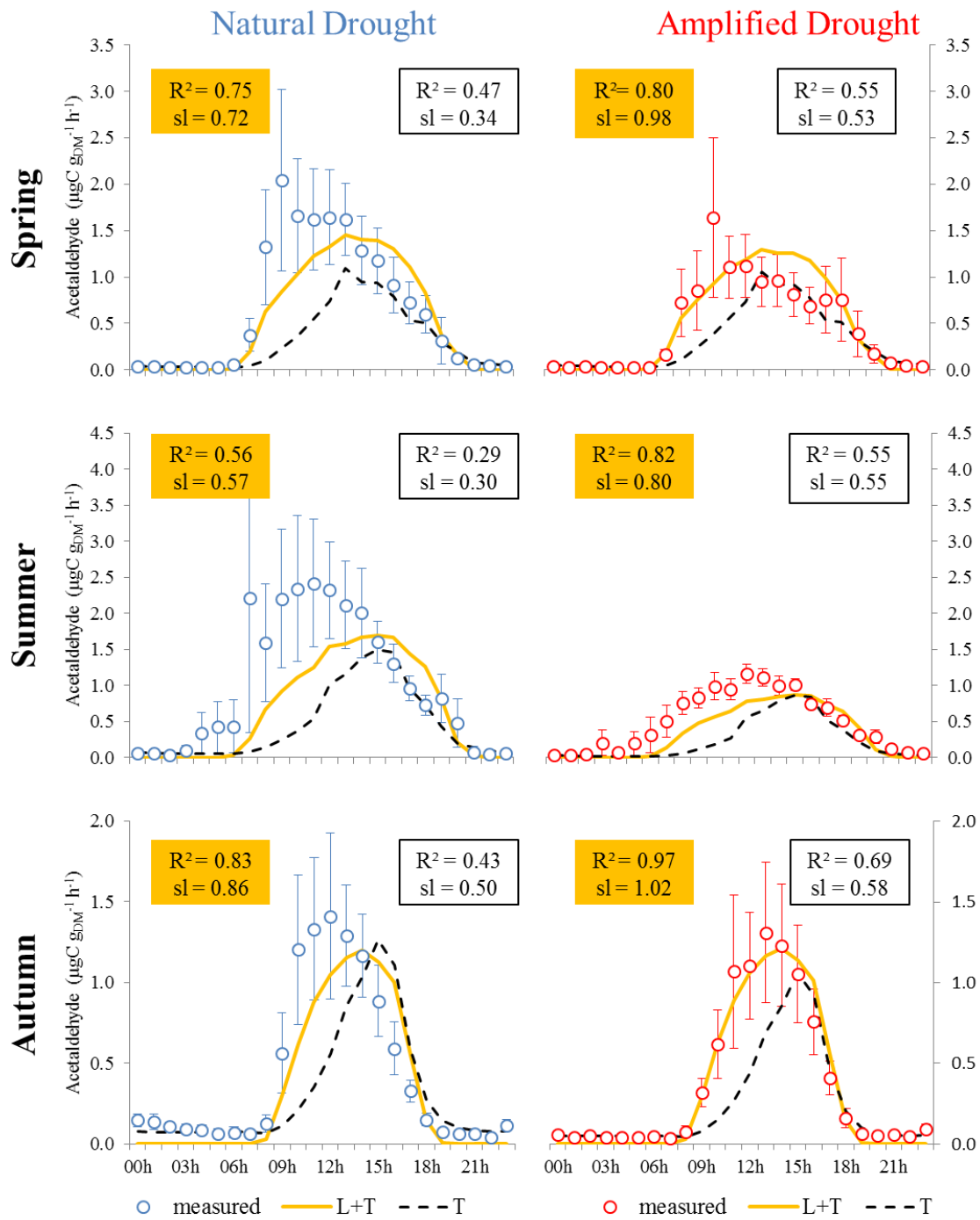


564

565 **Figure 3:**

566

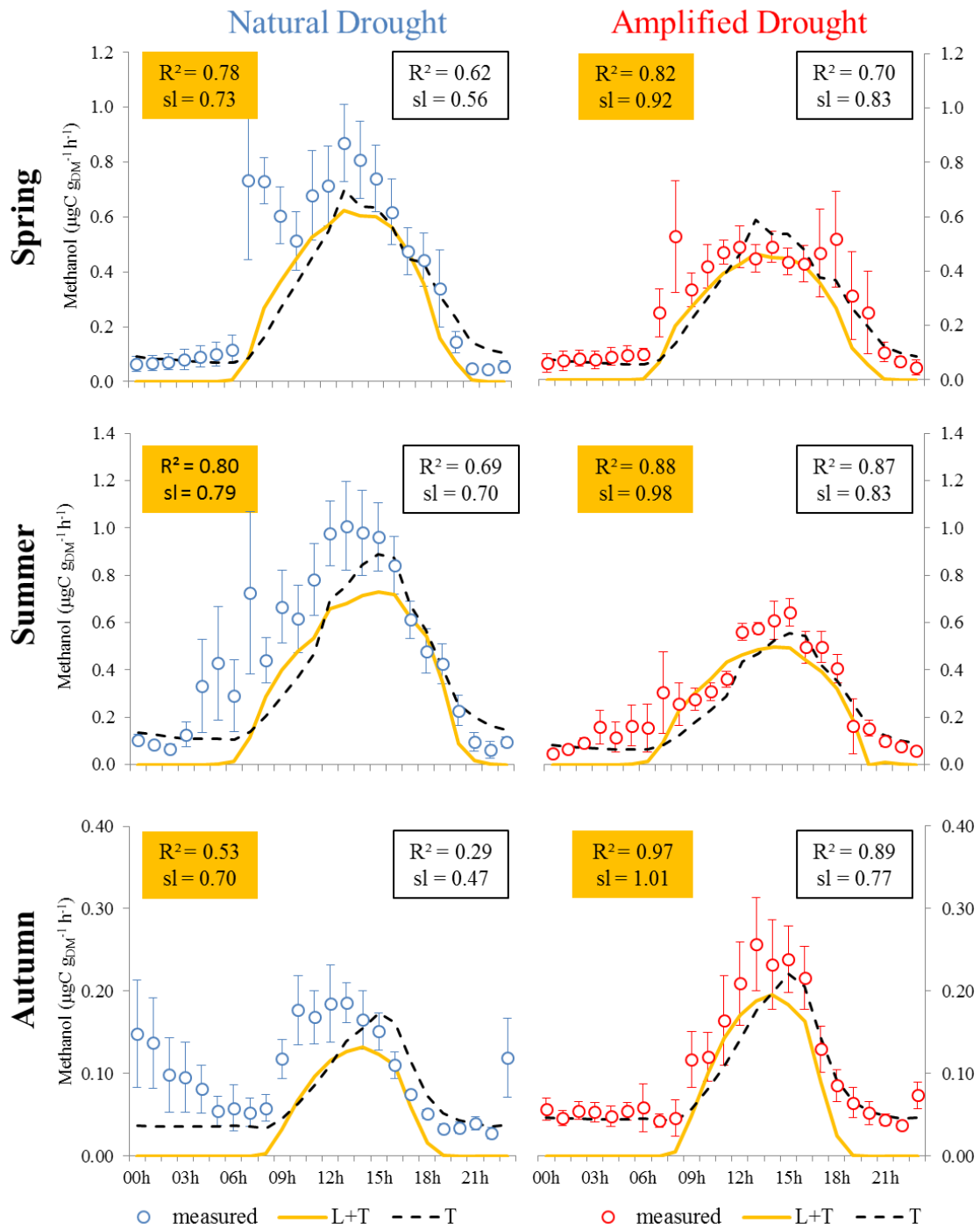
567



568

569 **Figure 4:**

570



571

572 **Figure 5:**

573

574

575

576

577